

Single-phase PV Generator Model for Distribution Feeders Considering Voltage Ride Through Conditions

L. G. O. Queiroz, O. E. Batista

Abstract—This paper presents a model for photovoltaic (PV) distributed generators that operates in abnormal electrical voltage scenarios - Voltage Ride Through (VRT), following the Brazilian standard NBR 16149 of 2013. The model includes various modes of operation, such as interruption of energy supply, disconnection, and reconnection of the PV system to the grid. Two types of simulations were performed to test the model's performance: the first involved using a ramp function to test the activation of different operating modes, while the second connected the PV model to a distribution feeder and tested its response to a short circuit. The results showed that the model met the requirements established by the standard and was efficient in representing the behavior of the PV system in real-world scenarios.

Keywords—Distributed generation. Photovoltaic system. NBR 16149. System modeling. Voltage ride through. Dynamic operation.

I. INTRODUCTION

CURRENTLY, the use of photovoltaic solar energy has been gaining considerable space, where the installed capacity has increased significantly all over the world. [1], [2], [3], [4]. In this context, the dynamic modeling of photovoltaic generators is characterized as an important tool to analyze DG performance in different scenarios. Although it is possible to find authors in the literature who present different types of models to represent PVDG, these methodologies generally have a complex level of implementation, compromising the analysis of scenarios with high penetration of DG [5], [6], [7], [8].

In addition, the high penetration of utility interconnected photovoltaic systems is leading to a need for systems to include grid support functions, to minimize the negative impact these variable distributed energy resources may have on system voltage and frequency [9]. Those functions include the Voltage Ride Through (VRT) and Frequency Ride-Through (FRT) parameters that refer to the ability to withstand voltage and frequency disturbances within defined limits and continue operating according to predetermined specifications. Thus, it becomes necessary that the modeling of distributed generation systems include such functions, allowing the proper operation of the generation system in the face of disturbances that affect the voltage levels. However, the literature presents few studies considering the ability of VRT and FRT in grids with high

numbers or high penetration of DGs, especially with regard to recommendations of Brazilian standards. The studies carried out in [10], [11], [12], [13], for example, model systems considering VRT conditions, but are not directed towards regulations of Brazilian concessionaires.

The requirement for parameters related to the operation of photovoltaic systems may have different characteristics, depending on the regulatory body in each country. In Brazil, Regulatory Standard (RS) 16149 of 2013 [14] establishes criteria for the connection interface with the distribution grid. Through limits assigned to voltage levels, ranges are defined for interrupting the energy supply by the DG, as well as its disconnection and reconnection of the DG to the grid.

Given the importance of the considerations made and using RS 16149 as a reference, this paper proposes a modeling of photovoltaic generators that considers the requirements for interrupting the energy supply by the DG and its possible disconnection or reconnection in the face of disturbances that affect the levels of electrical voltage. In addition, the modeling of the photovoltaic generator is carried out in a simplified way, aiming at a better implementation strategy in scenarios with high DG integration.

II. THE BRAZILIAN REGULATORY STANDARD 16149 (2013)

A. Scope

The standard RS 16149 of 2013 provides recommendations for the connection interface between photovoltaic systems and the power distribution grid, specifying their requirements. It outlines guidelines for the operation of the photovoltaic system based on voltage and frequency values, which include interrupting energy supply, reducing or increasing supplied power, and disconnecting the DG from the grid.

B. Recommendations to Voltage Variation - Voltage Ride-through (VRT)

According to RS 16149, when the nominal voltage of the grid leaves the operating range specified in Table I, the photovoltaic system must stop supplying energy to the grid, regardless of whether the system is single-phase or polyphase. Therefore, the photovoltaic system must perceive an abnormal voltage condition and act, ceasing supply to the grid, but remaining connected to the grid.

In Table I, the maximum supply interruption time refers to the time between the abnormal voltage event and the

This study was financed in part by the Coordenação de Aperfeiçoamento de Pessoal de Nível Superior - Brazil (CAPES) -Finance Code 001.

Paper submitted to the International Conference on Power Systems Transients (IPST2023) in Thessaloniki, Greece, June 12-15, 2023.

TABLE I
CONDITIONS FOR SHUTDOWN UNDER ABNORMAL VOLTAGE CONDITIONS

Voltage at the point of common connection (V_{PCC})	Maximum supply interruption time
$V_{PCC} > 1.1$ pu	0.2s
0.8 pu $\leq V_{PCC} \leq 1.1$ pu	Normal Operation
$V_{PCC} < 0.8$ pu	0.4s

Source: Adapted from [14]

stop of supplying energy to the grid. The photovoltaic system must remain connected to the grid in order to monitor the grid parameters and allow the re-supply of power when normal conditions are restored. In addition to the shutdown recommendations presented in Table I, RS 16149 provides conditions for PVDG disconnection (Table II). Such requirements aim to avoid undue disconnection of the network in cases of voltage sag, ensuring the withstand to under voltages resulting from faults in the network.

TABLE II
WITHSTANDABILITY REQUIREMENTS FOR UNDER VOLTAGES DUE TO FAULTS ON THE NETWORK

Voltage at the point of common connection (V_{PCC})	Minimum disconnection time
0.8 pu $\leq V_{PCC} \leq 1.1$ pu	Normal Operation
$0.4 \leq V_{PCC} \leq 0.8$ pu	0.3s
$V_{PCC} < 0.4$ pu	0.2s

Source: Adapted from [14]

In Table II, the minimum disconnection time refers the minimum time that the GD must operate under abnormal conditions so that its disconnection can be carried out.

In the case of a disconnection of the DG from the grid as a result of abnormal grid conditions, RS 16149 stipulates that the PV system cannot restart supplying electricity to the grid for a period of 20 to 300 seconds following the restoration of normal grid voltage and frequency.

III. PHOTOVOLTAIC GENERATOR MODELING

A. PVDG Modes of Operation

In view of the recommendations established by RS 16149 and previously presented, the proposed modeling of the photovoltaic generator started from the creation of different modes for operation and performance of the photovoltaic system connected to the grid, which consider the voltage measurements at the Common Coupling Point (PCC) and the grid frequency.

1) *Operating Modes for Voltage Variation:* Considering the conditions for interrupting the power supply (Table I) and for disconnecting the PVDG (Table II), seven different operating modes related to voltage in the PCC were created:

(a) **Mode 1: ($V_{PCC} > 1.1$ pu) and ($0.1s \leq T1 < 0.2s$)**

As described by RS 16149 and shown in Table I, the PVDG must remain connected to the grid for this voltage range, however it is allowed that the power supply is stopped. Furthermore, considering that the maximum

shutdown time should be 0.2s, it was fixed that this response should only occur if the voltage on the PCC remains greater than 1.1 pu for at least 0.1s and for less than 0.2s. The minimum time was established so that short-term disturbances do not cause interruptions in the power supply to the network, avoiding excessive and unnecessary disconnections. The $T1$ variable corresponds to the time the system remains with V_{PCC} above 1.1 pu.

(b) **Mode 2: ($V_{PCC} > 1.1$ pu) and ($T1 \geq 0.2s$)**

The second operating mode considers the same voltage range as Mode 1, however, in addition to interrupting the power supply, it also establishes DG disconnection. Disconnection must be carried out if the voltage abnormality remains for a period greater than or equal to 0.2 seconds ($T1 \geq 0.2s$).

(c) **Mode 3: ($0.8 \leq V_{PCC} \leq 1.1$ pu)**

In operating mode 3, the system is within the normal operating range. In this case, no action should be taken, and the PVDG should continue to supply energy until voltage levels exceed normal limits.

(d) **Mode 4: ($0.4 \leq V_{PCC} < 0.8$ pu) and ($0.2s \leq T2 < 0.4s$)**

When the V_{PCC} is between 0.4 pu and 0.8 pu for at least 0.2 s and for less than 0.4 s, the power supply from the photovoltaic system must be interrupted, but keeping the PV connected to the grid. Although RS 16149 recommends interrupting the power supply for any voltage lower than 0.8 pu (Table I), the voltage range between 0.4 pu and 0.8 pu was established in this operating mode with the intention that the PVDG shutdown is done before its disconnection: according to the Table II, there are different conditions of disconnection for voltages less than 0.8 pu and less than 0.4 pu. The $T2$ variable corresponds to the time the system remains with V_{PCC} at least 0.4 pu and less than 0.8 pu.

(e) **Mode 5: ($0.4 \leq V_{PCC} < 0.8$ pu) and ($T2 \geq 0.4s$)**

The Mode 5 considers the same voltage range as Mode 4, however, in addition to interrupting the power supply, it also establishes DG disconnection. Disconnection must be carried out if the voltage abnormality remains for a period greater than or equal to 0.4 seconds ($T2 \geq 0.4s$).

(f) **Mode 6: ($V_{PCC} < 0.4$ pu) and ($0.2s \leq T3 < 0.3s$)**

According to RS 16149, it was established that when the voltage is below 0.4 pu, the PVDG must stop supplying if it remains at this voltage level for a time ($T3$) of at least 0.2 seconds and less than 0.3 seconds. The DG's connection to the grid must be maintained for this time interval.

(g) **Mode 7: ($V_{PCC} < 0.4$ pu) and ($T3 \geq 0.3s$)**

As noted in the Table II, the photovoltaic system must be disconnected from the grid if V_{PCC} remains less than 0.4 pu for a minimum time of 0.2s. In this way, and considering the operating range of Mode 6, operation mode 7 establishes the disconnection of the PVDG if $T3 \geq 0.3$ seconds.

Through the seven established operating modes, the

recommendations of RS 16149 can be fulfilled for the performance of the distributed generation system connected to the grid in the face of voltage variation in the PCC. Thus, the developed distributed generator modeling will take into account each of the presented modes, and which are summarized in Table III, where the variable TR refers to the time required to reconnect the distributed system to the grid. After a disconnection, returning the electrical voltage levels to the normal operating range (Mode 3), for at least 20 seconds, the reconnection is allowed.

2) *Influence of the Operating Modes on the Active Power Provided by the PV Generator Connected to the Grid:* Through the operating modes for voltage, the power supplied by the PVDG can be stopped or reduced. Thus, the Equation 1 represents the respective values of Active Power (P_{pv}) considering the 7 operating modes previously described.

$$P_{pv} = \begin{cases} 0, & \text{if } (V_{PCC} > 1.1 \text{ pu}) \text{ and } (T1 \geq 0.1s) \\ 0, & \text{if } (0.4 \leq V_{PCC} < 0.8 \text{ pu}) \text{ and } (T2 \geq 0.2s) \\ 0, & \text{if } (V_{PCC} < 0.4 \text{ pu}) \text{ and } (T3 \geq 0.2s) \\ P_{nom}, & \text{if } (0.8 \leq V_{PCC} \leq 1.1 \text{ pu}) \end{cases} \quad (1)$$

B. Simplified Photovoltaic Generator Model (SPVM): Model for Normal Operating Conditions

In this section the Simplified Photovoltaic Generation Model (SPVM) is going to be described. Its development was carried out based on the conventional composition of the PV system: the PV generator; the power electronic converter between the dc and ac sides; and the components of the AC side (see Fig. 1).

With the aim of simplifying the model shown in Fig. 1, some considerations were made: the grid coupling transformer was ignored; the output filter just works for frequencies near and above the switching frequencies, so it was removed; and the resistance R_{dc} was omitted for being very small. Thus, a new diagram, that represent the simplified PV system is showed in Fig. 2.

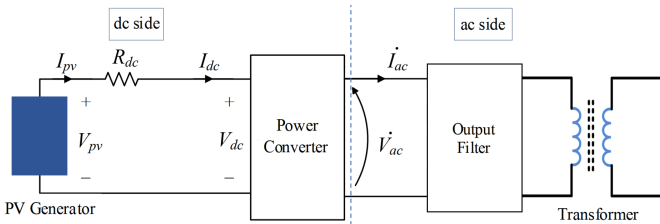


Fig. 1. Single-phase Grid-Connected Photovoltaic Generator Diagram.

The Fig. 3 showed the generator of the photovoltaic system, that can be represented as a Norton equivalent when considering all modules of the same type and subject to the same environmental conditions. The $I_{gen,eq}$ represents the equivalent current generated by the modules, and $R_{gen,eq}$ the model equivalent resistance, generally despised for being very high.

Regarding the power converter, it is assumed that it will be of the Grid-feeding type, represented by a current source

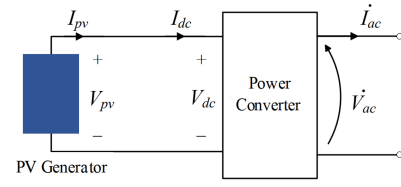


Fig. 2. Simplified Single-phase Grid-connected Photovoltaic Generator Diagram.

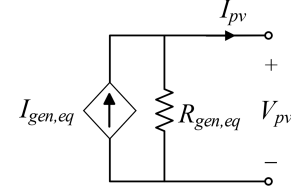


Fig. 3. Norton Equivalent Circuit of a PV Generator.

that controls the current injected into the PCC and performs the correct voltage modulation so that it is synchronized in frequency and amplitude with the grid. Thus, the voltage and the current, V_{ac} and I_{ac} , in Fig. 2, can be defined, in time domain, as (2) and (3), respectively:

$$v_{ac}(t) = v_{ac-peak} \cdot \cos(\omega t + \theta) = v_g(t) \quad (2)$$

$$i_{ac}(t) = i_{ac-peak} \cdot \cos(\omega t + \alpha) \quad (3)$$

Furthermore, according to the considerations made previously, and despising internal switching losses in the power converter, based on the principle of power balance, P_{pv} is equal to P_{ac} , thus:

$$P_{pv} = P_{ac} = \frac{V_{ac-peak} \cdot I_{ac-peak}}{2} \cos(\theta - \alpha) \quad (4)$$

Rearranging (4) and considering $\alpha = \theta - \arccos(pf)$, it is possible represents $I_{ac-peak}$, as (5).

$$I_{ac-peak} = \frac{2P_{pv}}{pf \cdot V_{ac-peak}} \quad (5)$$

Finally, combining (5) with (3), I_{ac} can be represented by

$$I_{ac}(t) = \frac{2P_{pv}}{pf \cdot V_{ac-peak}} \cos(\omega t + \alpha) \quad (6)$$

Depending on three main variables, the DG power supplied (P_{pv}), the power factor (pf) and the peak voltage ($V_{ac-peak}$), the modeling can be done more easily and requiring a lower level of processing. The estimation of the ω and α values in Equation 3 can be performed using the Phase-Locked Loop (PLL) technique, which synchronizes the power converter with the grid frequency, controlling the current injected into the PCC. In Fig. 4 is showed, the SPVM single-phase simulation in Matlab/Simulink. Matlab/Simulink was chosen for photovoltaic generator modeling due to its proven accuracy, reliability, and flexibility in handling nonlinear and complex systems. Additionally, its extensive modeling resources, and support for libraries make it an accessible option for users

after a PVDG power supply interruption. Another strategy was the inclusion of the "Keep mode 1" block depicted in Figure 6, which ensures that mode 1 remains active even if the current voltage levels do not meet its activation requirements. This approach prevents a zero output in the summing block. If the criteria for mode 1 are no longer met but the time required to switch to another mode is not reached, the system remains in the last mode attained. It should be noted that other operation mode blocks follow a similar strategy.

IV. ANALYSIS AND SIMULATION OF THE PROPOSED MODELING

In this section, the performance of the SPVM/CPVM is analyzed. Initially, two comparative studies were carried out to validate the simplified photovoltaic generator model (Figure 4). The first was carried out by comparing the SPVM with real generation data; the second was done by comparing the proposed model with another model already present in the literature. After the comparative studies, the performance of the model was verified for abnormal operating conditions.

A. SPVM \times Real photovoltaic plant

A comparative analysis was conducted between real data generated by a 150.8 kWp photovoltaic power plant, and estimated data obtained from the SPVM. The photovoltaic plant is located on the Mossoró campus of the Universidade Federal Rural do Semi-árido (RN, Brazil), and its generation data are freely available online. Thus, the energy generated in each month was calculated using the generation values corresponding to each hour of the year 2022, totaling 8760 different values of generated energy. Using the technical data of the real photovoltaic system (Table IV), a simulation was performed using the proposed model, and instantaneous power was obtained by measuring voltage and current, which in turn allowed for the estimation of the energy generated in each month. Meteorological data for the year 2022 corresponding to the location of the photovoltaic system was also utilized as input variables in the modeling. The results, as shown in Figure 7, demonstrate a high level of agreement between the real and modeled systems.

TABLE IV
GENERAL CHARACTERISTICS OF THE PLANT

Name	Mossoró 2
Local	UFERSA (Mossoró Campus)
Number of modules	580
Modules model	Canadian Solar CS6P260P-SD
Watt-peak module (Wp)	260
Total watt-peak module (kWp)	150.8
Connection type	On-grid

Figure 8 presents the percentage variation values between the real and estimated data over a period of one year. It can be seen that the estimated values closely follow the real values throughout the year, with a mean variation of 2,77%, and a maximum variation of 6.25% in September month. The results of the comparative study provide evidence of the effectiveness of the SPVM model in accurately representing the behavior of the photovoltaic system. Notably, the study

utilized different values of irradiance and temperature for each of the 8760 hours in a year, demonstrating the model's ability to account for the dynamic nature of environmental conditions and their impact on energy generation. This finding reinforces the reliability of the model and its potential for use in practical applications, such as the design and operation of photovoltaic power plants. It is worth noting that possible inaccuracies in the measurement of meteorological data, such as temperature and irradiance, can also impact the estimation of energy generation.

B. SPVM \times PV Array

The feeder shown in Fig. 9 was used to represent the distribution network in which the SPVM will be connected in the point of common coupling (PCC) to obtain the voltage, current, active, and reactive power values after integrating the distributed generator and considering now the presence of a single-phase short-circuit in the feeder. Subsequently using a feeder with the same characteristics mentioned above, aiming for a comparative study, dynamic simulations were performed using another PV generator model (PV Array) available at Simulink/MatLab. The distribution system is described in Tables V.

TABLE V
FEEDER DATA.

Parameter	Value
Voltage source (Vs)	240 $\angle 0^\circ$
Frequency (f)	60 Hz
Load 1	1000 + j500 VA
Load 2	2000 + j1000 VA
Load 3	1500 + j500 VA
Branches	$1.885 \times 10^{-3} + j2.5 \times 10^{-4}$

Initially, each model was simulated considering 12 different cases. The variation of irradiance level, and the use of arbitrary values of reactive current reference (I_q) generated different results for each simulation.

To allow a fair comparison between the results of each model, the values of Power Factor (pf) obtained from the PV Array model were inserted in the SPVM through the PF blocks (Fig. 4).

The results of the comparison between the models, with the relative error from the SPVM model, are presented in Figure 10, where can be concluded that the simplified model presents a high level of precision. For voltage and current, the maximum variation obtained did not exceed 3%, while for power levels, the variation was below 4% in all cases.

C. SPVM in abnormal conditions

After the comparative studies described, was investigated the activation of the operating modes designed for voltage regulation and transient response (VRT) conditions. By examining the behavior of the model in such conditions, we can gain a better understanding of its ability to accurately represent the behavior of the photovoltaic system in real-world scenarios. These findings have important implications for the

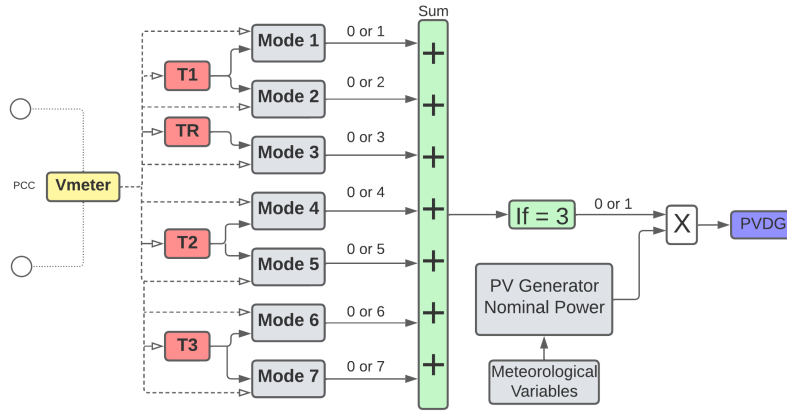


Fig. 5. VRT - Operation Modes Implementation Logic

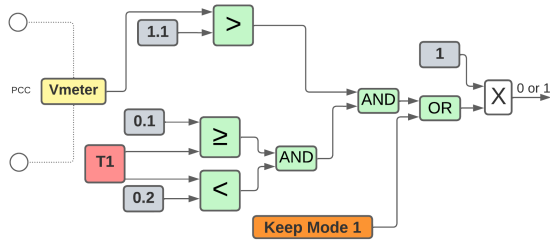


Fig. 6. VRT - Operation Mode 1

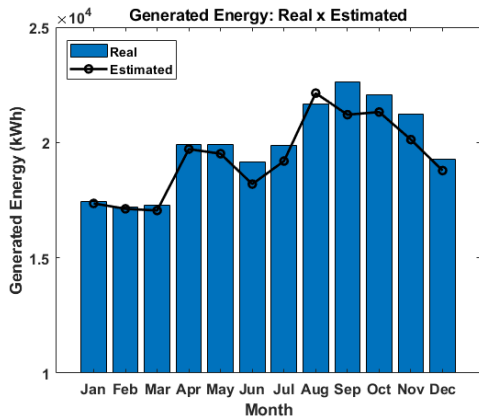


Fig. 7. Comparison between real values of generated energy and estimated values through the proposed model

practical application of the model in the design and operation of photovoltaic power plants. Thus, initially, a ramp function, which represents the electrical voltage in pu, will be used as input. In this way, from the variation of the values, the activation of different operating modes will occur, representing the interruption of energy supply by PVDG, its disconnection, or even its reconnection.

Following the use of the ramp function as an input variable, we will conduct a new analysis of the feeder shown in Figure 9. This time, we will use the voltage value measured at the point of common coupling (PCC) as the reference voltage. The analysis will be carried out in two stages: first, it will

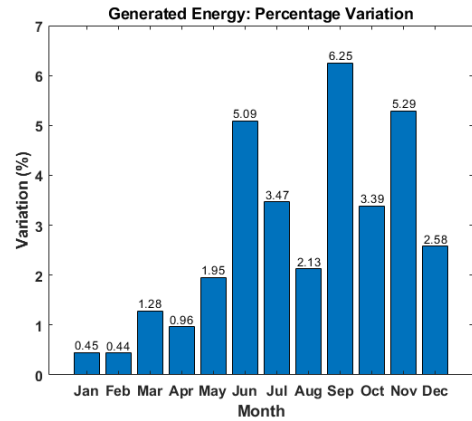


Fig. 8. Percentage change between real and estimated generation

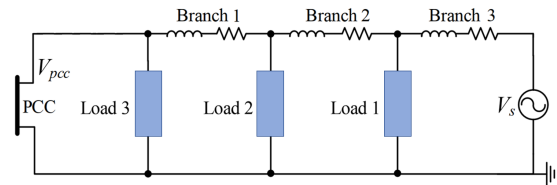


Fig. 9. Single-phase feeder

examine the normal operation of the feeder, with voltage and frequency levels within the standard operating range. In the second stage, we will introduce a single-phase fault at the PCC, causing changes in voltage and current levels that require the activation of the operating modes developed in Section III. This analysis will enable us to determine whether the proposed model meets the guidelines established by RS 16149 and can be used for dynamic analysis of distribution systems with photovoltaic distributed generation integration. The feeder's relevant data are presented in Table V.

1) *Analyses with Ramp Function:* As mentioned, the purpose of this first analysis is to verify whether the initialization of the operating modes is being carried out properly according to the input values. The ramp function will

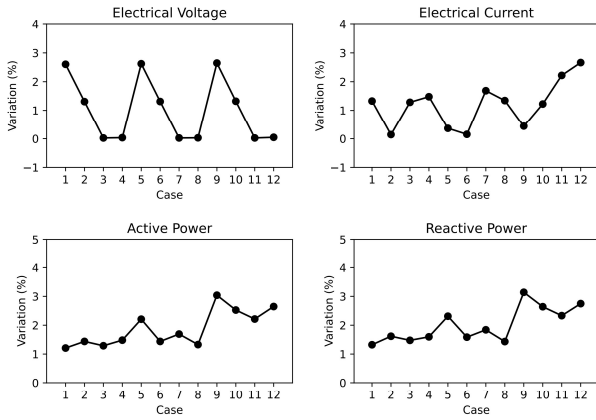


Fig. 10. Variation: SPVM x PV Array

provide input values that will vary between 0.15 and 1.65, reaching the different operating ranges shown in Table III.

Figure 11 presents the result obtained from the simulation that combined the input ramp with the processing of the seven operating modes.

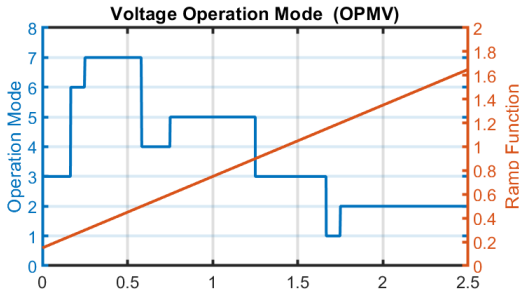


Fig. 11. Voltage Operation Mode - Ramp Function

The analysis of the results shown in Figure 11 can be done according to the operating mode active at each moment. In this way, its description will be made by stages, described below.

- 1) **Stage 1: Mode 3 activated**
At the beginning, operating mode 3 is activated. Despite the ramp function presenting values below 0.4, the system keeps mode 3 activated until the minimum time ($T_3 = 0.2s$) for activating mode 6 is reached.
- 2) **Stage 2: Mode 6 activated**
After the input value remains below 0.4 for 0.2s, the change from operating mode 3 to 6 occurs, representing an interruption of the energy supply by the PVDG.
- 3) **Stage 3: Mode 7 activated**
Still within the same voltage range as the previous stage, mode 7 is activated when T_3 reaches 0.3s, indicating the disconnection of the PVDG to the grid.
- 4) **Stage 4: Mode 7 stays on**
In this stage, the ramp function starts to reach values greater than 0.4, but the system keeps operating mode 7 active, since T_2 is less than 0.2s.
- 5) **Stage 5: Mode 4 activated**
Operating mode 4 is activated as the input value remains between 0.4 and 0.8 for more than 0.2s and for less

than 0.4s. Although mode 4 does not represent PVDG disconnection, the system remains disconnected from the grid due the activation of mode 7 in the previous stage.

- 6) **Stage 6: Mode 5 activated**
Switching from operating mode 4 to 5 when $T_2 = 0.4s$.
- 7) **Stage 7: Mode 5 stays on**
Input value reaches the normal operating range (between 0.8 and 1.1), but keeps operating mode 5 active until the minimum time for reconnecting the PVDG to the grid is reached.
- 8) **Stage 8: Mode 3 activated**
The minimum time for reconnection is reached and the DG reconnects to the grid again. Despite the minimal time for reconnection (TR be 20s, according to Table III, a TR value equal to 0.1 was used in the simulation to facilitate the analysis.
- 9) **Stage 9: Mode 3 stays on**
The value of the ramp function exceeds 1.1. The system will keep the previous operating mode active until this range remains for at least 0.1s
- 10) **Stage 10: Mode 1 activated**
 T_1 reaches 0.1s and mode 1 is activated. PVDG again interrupts the power supply to the grid.
- 11) **Stage 11: Mode 2 activated**
 T_1 exceeds 0.2s and operation mode 2 is activated, representing the PVDG disconnection.

D. Analyses with Feeder

The results below show how the system works after connecting the PVDG to the distribution feeder shown in Figure 9.

- 1) **Analysis for Feeder with Normal Voltage Conditions:**
For normal operating conditions with a $P_{nom} = 3500$ W, the Figure 12 represents the active operating mode and the power supplied by the PVDG over time.

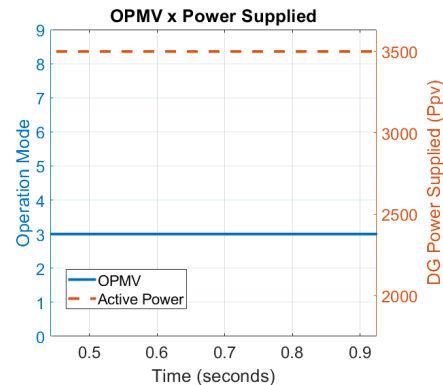


Fig. 12. Voltage Operation Mode (OPMV) and DG Power Supplied - Normal Conditions

For the system's normal operation (electrical voltage close to 1 pu), operating mode 3 remains always activated, with no need to interrupt the power supply by the P_{PV} , nor to perform its disconnection. With mode 3 active, the supplied power remains constant and equal to P_{nom} (Figure12).

2) *Analysis for Feeder with Abnormal Voltage and Conditions:* After the analysis for normal operating conditions, a short circuit was introduced to the feeder between 0.3s e 0.8s. Thus, the system starts to show significant variations in voltage and current levels (Figure 13).

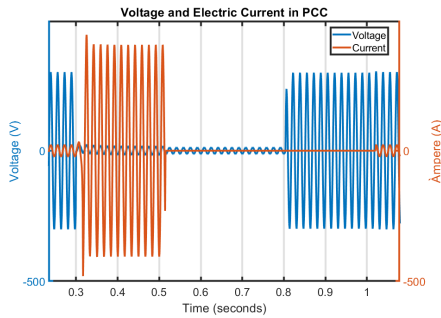


Fig. 13. Voltage and Current in the PCC - Abnormal Conditions

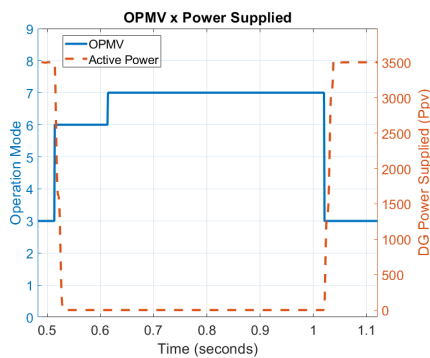


Fig. 14. Voltage Operation Mode (OPMV) and DG Poweer Supplied - Abnormal Conditions

Figure 14 shows the different active operating modes over time. Initially, operation mode 3 is active until the short circuit lasts for the minimum time necessary to activate another mode. When the short circuit begins at 0.3 seconds and considering T3's minimum time of 0.2 seconds, operation mode 6 is activated at 0.5 seconds. The switch from mode 3 to mode 6 is due to the low voltage values in the PCC falling below 0.4 pu. The activation of operation mode 6 indicates the interruption of the energy supply, causing null values of active power and electric current, as can be seen in Figures 14 and 13, respectively. After spending at least 0.3s with the PCC voltage below 0.4 pu, the active operating mode changes from mode 6 to 7. In this new scenario, the PVDG becomes disconnected from the grid (the supplied power remains equal to zero), and its reconnection can only be performed after meeting the conditions established for operating mode 3. Finally, the system returns to normal voltage values after the short circuit is interrupted at 0.8s. However, the PVDG is only reconnected after reaching the minimum time under normal operating conditions, which was fixed at 0.2s to facilitate analysis. The PVDG supplies energy when the simulation reaches 1s.

V. CONCLUSIONS

The paper presents a model for distributed photovoltaic generators (PVDGs) compliant with Brazilian standard NBR

16149, specifically for voltage ride through (VRT) conditions. With seven operating modes, the model dynamically interrupts and reconnects power supply from the PVDG to the grid. This model can be used to study scenarios with voltage abnormalities caused by faults, offering more precise analyses of PVDG's impact on the distribution network. The simplified generator model is computationally efficient and easy to implement. Although the model is currently limited to VRT conditions, future updates will include frequency ride-through (FRT) to provide a more comprehensive analysis of PVDG performance. The initial model can be used for voltage variation analyses in the point of common coupling (PCC), resulting in a simpler yet effective model for the intended objectives.

REFERENCES

- [1] N. Haghdadi, A. Bruce, I. MacGill, and R. e Passey, "Impact of distributed photovoltaic systems on zone substation peak demand," *IEEE Transactions on Sustainable Energy*, vol. 9, no. 2, pp. 621–629, 2018.
- [2] S. Matos, M. Vargas, L. Fracalossi, L. Encarnação, and O. Batista, "Protection philosophy for distribution grids with high penetration of distributed generation," *Electric Power Systems Research*, vol. 196, p. 107203, 2021.
- [3] D. Cheng, B. A. Mather, R. Seguin, J. Hambrick, and R. P. Broadwater, "Photovoltaic (pv) impact assessment for very high penetration levels," *IEEE Journal of Photovoltaics*, vol. 6, no. 1, pp. 295–300, 2016.
- [4] B. R. Baroni, W. Uturbey, A. M. G. Costa, and S. P. Rocha, "Impact of photovoltaic generation on the allowed revenue of the utilities considering the lifespan of transformers: A brazilian case study," *Electric Power Systems Research*, vol. 192, p. 106906, 2021.
- [5] Vinod, R. Kumar, and S. Singh, "Solar photovoltaic modeling and simulation: As a renewable energy solution," *Energy Reports*, vol. 4, pp. 701–712, 2018.
- [6] A. Bouraiou, M. Hamouda, A. Chaker, M. Sadok, M. Mostefaoui, and S. Lachtar, "Modeling and simulation of photovoltaic module and array based on one and two diode model using matlab/simulink," *Energy Procedia*, vol. 74, pp. 864–877, 2015, the International Conference on Technologies and Materials for Renewable Energy, Environment and Sustainability ?TMREES15.
- [7] J. Seuss, M. J. Reno, R. J. Broderick, and S. Grijalva, "Determining the impact of steady-state pv fault current injections on distribution protection," 2017.
- [8] M. M. El-Saadawi, A. E. Hassan, K. M. Abo-Al-Ez, and M. S. Kandil, "A proposed framework for dynamic modelling of photovoltaic systems for dg applications," *International Journal of Ambient Energy*, vol. 32, no. 1, pp. 2–17, 2011.
- [9] M. Ropp, D. Schultz, J. Neely, and S. Gonzalez, "Effect of grid support functions and vrt/frt capability on autonomous anti-islanding schemes in photovoltaic converters," in *2016 IEEE 43rd Photovoltaic Specialists Conference (PVSC)*, 2016, pp. 1853–1856.
- [10] A. Pandey and A. Singh, "Svrdf controller for single phase grid tied pv system with low voltage ride through capability," *Electric Power Systems Research*, vol. 214, p. 108878, 2023. [Online]. Available: <https://www.sciencedirect.com/science/article/pii/S0378779622009312>
- [11] Y. Geng, K. Yang, Z. Lai, P. Zheng, H. Liu, and R. Deng, "A novel low voltage ride through control method for current source grid-connected photovoltaic inverters," *IEEE Access*, vol. 7, pp. 51 735–51 748, 2019.
- [12] A. Merabet, L. Labib, and A. M. Y. M. Ghias, "Robust model predictive control for photovoltaic inverter system with grid fault ride-through capability," *IEEE Transactions on Smart Grid*, vol. 9, no. 6, pp. 5699–5709, 2018.
- [13] H. Dai, C. L. Ruan, C. H. Yan, W. Z. Huang, Y. C. Wu, and L. X. Sun, "Impact of fault ride-through characteristics of large-scale distributed photovoltaic integration on voltage in receiving-end grid," in *2022 IEEE 5th International Electrical and Energy Conference (CIEEC)*, 2022, pp. 3137–3141.
- [14] ABNT, *Sistemas fotovoltaicos (FV): Características da interface de conexão com a rede elétrica de distribuição*, Março 2013.